https://doi.org/10.1093/brain/awab282 BRAIN 2022: 145; 340–348 | 340

BRAIN
ORIGINAL ARTICLE

Molecular pathology and synaptic loss in primary tauopathies: an ^{18}F-AV-1451 and ^{11}C-UCB-J PET study

Negin Holland,[1,2] Maura Malpetti,[1] Timothy Rittman,[1,2] Elijah E. Mak,[3] Luca Passamonti,[1,4] Sanne S. Kaalund,[1] Frank H. Hezemans,[1,5] P. Simon Jones,[1] George Savulich,[3] Young T. Hong,[6] Tim D. Fryer,[1,6] Franklin I. Aigbirhio,[1] John T. O'Brien[2,3] and James B. Rowe[1,2,5]

The relationship between *in vivo* synaptic density and molecular pathology in primary tauopathies is key to understanding the impact of tauopathy on functional decline and in informing new early therapeutic strategies. In this cross-sectional observational study, we determine the *in vivo* relationship between synaptic density and molecular pathology in the primary tauopathies of progressive supranuclear palsy and corticobasal degeneration as a function of disease severity.

Twenty-three patients with progressive supranuclear palsy and 12 patients with corticobasal syndrome were recruited from a tertiary referral centre. Nineteen education-, sex- and gender-matched control participants were recruited from the National Institute for Health Research 'Join Dementia Research' platform. Cerebral synaptic density and molecular pathology, in all participants, were estimated using PET imaging with the radioligands ^{11}C-UCB-J and ^{18}F-AV-1451, respectively. Patients with corticobasal syndrome also underwent amyloid PET imaging with ^{11}C-PiB to exclude those with likely Alzheimer's pathology—we refer to the amyloid-negative cohort as having corticobasal degeneration, although we acknowledge other underlying pathologies exist. Disease severity was assessed with the progressive supranuclear palsy rating scale; regional non-displaceable binding potentials of ^{11}C-UCB-J and ^{18}F-AV-1451 were estimated in regions of interest from the Hammersmith Atlas, excluding those with known off-target binding for ^{18}F-AV-1451. As an exploratory analysis, we also investigated the relationship between molecular pathology in cortical brain regions and synaptic density in subcortical areas.

Across brain regions, there was a positive correlation between ^{11}C-UCB-J and ^{18}F-AV-1451 non-displaceable binding potentials ($\beta = 0.4$, $t = 3.6$, $P = 0.001$), independent of age or time between PET scans. However, this correlation became less positive as a function of disease severity in patients ($\beta = -0.02$, $t = -2.9$, $P = 0.007$, $R = -0.41$). Between regions, cortical ^{18}F-AV-1451 binding was negatively correlated with synaptic density in subcortical areas (caudate nucleus, putamen). Brain regions with higher synaptic density are associated with a higher ^{18}F-AV-1451 binding in progressive supranuclear palsy/corticobasal degeneration, but this association diminishes with disease severity. Moreover, higher cortical ^{18}F-AV-1451 binding correlates with lower subcortical synaptic density. Longitudinal imaging is required to confirm the mediation of synaptic loss by molecular pathology. However, the effect of disease severity suggests a biphasic relationship between synaptic density and molecular pathology with synapse-rich regions vulnerable to accrual of pathological aggregates, followed by a loss of synapses in response to the molecular pathology. Given the importance of synaptic function for cognition and action, our study elucidates the pathophysiology of primary tauopathies and may inform the design of future clinical trials.

Received March 02, 2021. Revised July 02, 2021. Accepted July 10, 2021. Advance access publication August 16, 2021

1 Department of Clinical Neurosciences, University of Cambridge, Cambridge Biomedical Campus, Cambridge CB2 0SZ, UK
2 Cambridge University Hospitals NHS Foundation Trust, Cambridge CB2 0QQ, UK
3 Department of Psychiatry, University of Cambridge, School of Clinical Medicine, Cambridge Biomedical Campus, Cambridge CB2 0QQ, UK
4 Istituto di Bioimmagini e Fisiologia Molecolare (IBFM), Consiglio Nazionale delle Ricerche (CNR), 20090 Milano, Italy
5 Medical Research Council Cognition and Brain Sciences Unit, University of Cambridge, Cambridge CB2 7EF, UK
6 Wolfson Brain Imaging Centre, University of Cambridge, Cambridge CB2 0QQ, UK

Correspondence to: Dr Negin Holland, MRCP, PhD
Association of British Neurologists Clinical Research Fellow, University of Cambridge
Herschel Smith Building, Robinson Way, Cambridge CB2 0SZ, UK
E-mail: nda26@cam.ac.uk

Keywords: primary tauopathies; PSP; CBD/CBS; synapse; tau

Abbreviations: BP_{ND} = non-displaceable binding potential; CBD = corticobasal degeneration; CBS = corticobasal syndrome; PSP = progressive supranuclear palsy–Richardson's syndrome

Introduction

Synaptic loss is a feature of many neurodegenerative disorders.[1–3] It is closely related to cognitive decline in symptomatic stages of disease,[4,5] but can begin long before symptom onset and neuronal loss.[6] Synaptic loss and dysfunction may be an important mediator of decline even where atrophy is minimal or absent.[7,8] Conversely, synaptic connectivity may facilitate the spread of oligomeric misfolded proteins such as tau.[9–14] The relationship between synaptic loss and the accumulation of misfolded proteins in primary tauopathies has yet to be determined *in vivo*. Preclinical models suggest early synaptotoxicity of oligomeric tau, leading to reduced synaptic plasticity and density.[15,16] In patients with mutations of microtubule-associated protein tau (MAPT), there are deficiencies in many synaptic pathways including GABA-mediated signalling and synaptic plasticity.[17] The mechanisms of synapse loss following tau pathology include both direct and indirect pathways (reviewed by Spires-Jones and Hyman[18]); however, the severity of synaptic toxicity in the related tauopathy of Alzheimer's disease appears to be dependent on the stage of disease in preclinical models and in patients post-mortem and *in vivo*. In animal models of Alzheimer's disease, and at human post-mortem, there is differential expression of synaptic proteins in the early stages with increases in some proteins and reductions in others.[19,20] This may be an attempt to maintain cellular physiology in early disease, which fails as the disease progresses, leading to loss of synaptic function and synapse numbers in moderate and advanced disease. In clinical disorders, the *in vivo* pathologies of synaptic density and tau burden can be characterized by PET. Recent *in vivo* PET imaging in Alzheimer's disease using ^{11}C-UCB-J as a marker of synaptic density and ^{18}F-AV-1451 or ^{18}F-MK-6240 PET as markers of tau pathology have shown decreased temporal lobe synaptic density with increasing pathological burden,[21] but with individual variability depending on the severity of cortical pathology.[22] However, the pathology of Alzheimer's disease is multifaceted with amyloid and tau aggregation, vascular changes and neuroinflammation.[23]

In this study, we use progressive supranuclear palsy–Richardson's syndrome (PSP)[24] and corticobasal degeneration (CBD)[25] as models of human tauopathy, with relevance to other tau-mediated neurodegenerative disorders, and examine the *in vivo* relationship between synaptic density and burden of molecular pathology. An advantage of studying PSP is the very high correlation between the clinical syndrome, and the specific 4R-tauopathy at autopsy.[26,27] The clinical phenotype of corticobasal syndrome (CBS), may be caused by CBD, but can also be mimicked by Alzheimer's disease and less commonly by other forms of frontotemporal lobar degeneration. Here, we use the term CBD to refer to patients with CBS in whom Alzheimer's disease is excluded by ^{11}C-PiB PET, whereby in the absence of amyloid pathology there is a high clinicopathological correlation with 4R-tauopathy at post-mortem. Both PSP and CBD demonstrate synaptic loss *in vivo*[7,8] and at post-mortem examination.[1,2] The distribution of tau pathology in both diseases is well characterized with cortical and subcortical involvement.[28,29] Animal models of tauopathy have illustrated the co-localization of tau aggregates at the synaptic bouton, associated with synaptic dysfunction and synaptic loss[18,30] but the tau–synapse association is yet to be determined *in vivo*. ^{18}F-AV-1451 signals are above normal in the cortex of patients with PSP and CBS/CBD,[31–37] but there is relatively low affinity for 4R-tauopathy compared to Alzheimer's disease, and off-target binding particularly in the basal ganglia. We therefore refer to ^{18}F-AV-1451 as a marker of 'molecular pathology', referring to the combination of tau and non-tau targets.

Figure 1 illustrates our hypotheses. Previous studies suggest that the strength of connectivity within a region and between brain regions can promote the spread of tau pathology, in humans as in preclinical models.[9–14] Therefore, we hypothesized that brain areas with higher synaptic density would develop more tau pathology (schematically represented by green arrows in Fig. 1A). We predicted that the spatial distribution of molecular pathology, as measured with the PET radioligand ^{18}F-AV-1451, would be correlated with synaptic density, as measured with the PET radioligand ^{11}C-UCB-J (which binds to the presynaptic vesicle glycoprotein SV2A that is ubiquitously expressed in brain synapses[38,39]). Because pathology in a region may impair efferent projections, a corollary hypothesis is that tau accumulation in one region (source region) leads to diaschisis characterized by reduced synaptic density in the areas to which it connects (target regions).

A second part of the model describes the consequence of the pathology, which is to reduce synaptic density (schematically represented by red arrows in Fig. 1A). The predicted result is a positive relationship between ^{18}F-AV-1451 binding and synaptic loss, negatively moderated by disease severity (Fig. 1B).

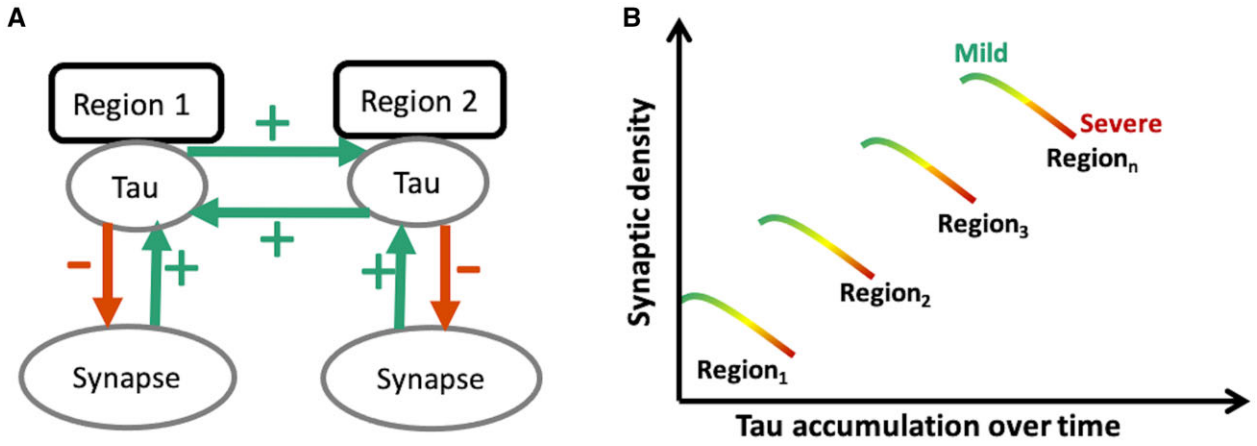

Figure 1 Schematic diagram illustrating the predicted toxic effect of tau on synaptic density as a function of disease severity. At a regional level (**A**) synaptic density promotes the spread of tau within the region, but also from one region to another functionally connected region (for example from Region 1 to Region 2 or vice versa; depicted by green arrows). However, tau is toxic to synapses, such that at a regional level it leads to a loss of synapses as the disease progresses. (**B**) Tau burden within a given region therefore depends on a region's baseline synaptic density: for example, Region 3, with a high baseline synaptic density, would accumulate more tau in the mild stages of disease (green); but as the disease progresses over time, to moderate and advanced stages (yellow and red, respectively), with increasing tau accumulation, tau-induced synapto-toxicity occurs with a decline in the number of synapses within any given region. Therefore, the prediction would be that, while in mild disease the degree of tau accumulation is dependent on baseline synaptic density, as the disease progresses this relationship breaks down, moving towards a negative association between tau accumulation and synaptic density.

Table 1 Clinical and demographics summary

	Control	PSP	CBD	*F*(*P*)
Gender, male:female	11:8	10:13	7:5	ns[a]
Age at ^{11}C-UCB-J PET in years	68.9 (7.1)	71.3 (8.6)	70.9 (7.9)	ns
Symptom duration, years	–	3.9 (2.2)	3.9 (2.1)	ns
Education, years	13.6 (2.8)	12 (4.2)	12.6 (2.8)	ns
ACE-R total (max. 100)	96.7 (2.7)	80.9 (12.4)	77.5 (17.1)	10.1 (<0.001)
Attention_Orientation (max 0.18)	17.9 (0.3)	16.3 (1.9)	16.3 (2.3)	4.5 (0.02)
Memory (max 0.26)	24.6 (1.7)	21.8 (3.8)	20.9 (5.3)	5.3 (0.01))
Fluency (max 0.14)	12.8 (1.0)	6.6 (3)	7.2 (3.5)	28.0 (<0.001)
Language (max 0.26)	25.6 (0.8)	23.3 (4.2)	21 (7.2)	5.4 (0.01)
Visuospatial (max 0.16)	15.7 (0.6)	12.8 (3.4)	12.1 (4.6)	7.5 (0.001)
MMSE (max. 30)	29.4 (1.2)	26.9 (2.6)	25.3 (4.9)	6.7 (0.002)
INECO (max. 30)	25.7 (2.1)	17.2 (5.4)	15.4 (6.5)	17.9 (<0.0001)
PSPRS (max. 100)	–	32.7 (8.2)	28.9 (10.0)	3.4 (0.07)
CBFS (max. 120)	–	32.7 (15.9)	26.2 (16.2)	0.2 (0.7)
Injected activity, MBq				
^{11}C-UCB-J	370.7 (114.3)	322.2 (86.0)	320.4 (113.8)	ns
^{18}F-AV-1451	182.3 (10.8)	182.1 (11.4)	186.1 (11.1)	ns
^{11}C-UCB-J and ^{18}F-AV-1451 PET scan interval, in days	157.2 (125.6)	155.9 (129.2)	45.5 (65.7)	4.6 (0.02)

Results are given as mean (and standard deviation) unless otherwise stated. PSP refers to patients with PSP–Richardson's syndrome. CBD refers to amyloid negative corticbasal syndrome. The *F*-statistic and *P*-values are derived from ANOVA. ACE-R = revised Addenbrooke's Cognitive Examination; CBFS = Cortical Basal ganglia Functional Scale; INECO = Institute of Cognitive Neurology frontal screening tool; MMSE = Mini-Mental State Examination; PSPRS = Progressive Supranuclear Palsy Rating Scale.
[a]Chi-squared test. ns = non-significant at $P < 0.05$.

Materials and methods

Participant recruitment and study design

Twenty-three patients with probable PSP–Richardson syndrome and 12 with probable CBS in whom Alzheimer's disease was excluded with ^{11}C-PiB PET were recruited from a regional specialist National Health Service clinic at the Cambridge University Centre for Parkinson-plus. We refer to our amyloid-negative CBS cohort as having CBD but acknowledge other pathologies are possible. Nineteen healthy volunteers were recruited from the UK National Institute for Health Research Join Dementia Research register. Participants were screened using the inclusion/exclusion criteria set out in Holland *et al.*[8] Eligible participants underwent clinical and cognitive assessments (Table 1) including the revised Addenbrooke's Cognitive Examination (ACE-R), the Mini-Mental State Examination (MMSE), and the Institute of Cognitive Neurology (INECO) frontal screening; disease severity was measured with the PSP rating scale, and the Cortical Basal ganglia Functional Scale.[40] Participants underwent 3 T MRI, ^{18}F-AV-1451 PET and ^{11}C-UCB-J PET. The research protocol was approved by the Cambridge Research Ethics Committee (reference 18/EE/0059) and the Administration of Radioactive Substances Advisory

Committee. All participants provided written informed consent in accordance with the Declaration of Helsinki.

PET data acquisition and kinetic analysis

^{11}C-UCB-J PET

The procedure for ^{11}C-UCB-J synthesis, PET data acquisition, image reconstruction and kinetic analysis was the same as in Holland *et al.*[8] In brief, dynamic PET data acquisition was performed on a GE SIGNA PET/MR (GE Healthcare) for 90 min immediately after injection, with attenuation correction using a multisubject atlas method[41] and improvements to the MRI brain coil component.[42] Emission image series were aligned using SPM12 (www.fil.ion.ucl.ac.uk/spm/software/spm12/) and rigidly registered to the T_1-weighted MRI acquired during PET data acquisition (repetition time = 3.6 ms, echo time = 9.2 ms, 192 sagittal slices, in plane resolution 0.55 × 0.55 mm, interpolated to 1.0 × 1.0 mm; slice thickness 1.0 mm). The Hammersmith atlas (http://brain-development.org) with modified posterior fossa regions was spatially normalized to the T_1-weighted MRI of each participant using advanced normalization tools software.[43] Regional time–activity curves were extracted following the application of geometric transfer matrix (GTM) partial volume correction (PVC[44]) to each dynamic PET image. Regions of interest were multiplied by a binary grey matter mask (>50% on the SPM12 grey matter probability map smoothed to PET spatial resolution), with the exception of the subcortical grey matter regions pallidum, substantia nigra, pons and medulla. To assess the impact of PVC, time–activity curves were also extracted from the same regions of interest without the application of GTM PVC (discussed below as 'without partial volume correction').

To quantify SV2A density, ^{11}C-UCB-J non-displaceable binding potential (BP_{ND}) was determined using a basis function implementation of the simplified reference tissue model,[45] with the reference tissue defined in the centrum semiovale.[46,47]

^{18}F-AV-1451 PET

As for ^{11}C-UCB-J, PET data acquisition was performed on a GE SIGNA PET/MR for 90 min after ^{18}F-AV-1451 injection, with attenuation correction as described above for ^{11}C-UCB-J. Image processing was also as given above for ^{11}C-UCB-J, except that ^{18}F-AV-1451 BP_{ND} was determined using a different basis function implementation of the simplified reference tissue model[48] and the reference tissue was defined in inferior cerebellar grey matter using a 90% threshold on the grey matter probability map produced by SPM12 smoothed to PET resolution.

^{11}C-PiB PET

Amyloid imaging using Pittsburgh Compound B (^{11}C-PiB) followed the protocol given in Holland *et al.*[8] ^{11}C-PiB cortical standardized uptake value ratio (SUVR; 50–70 min post injection) was calculated using the whole cerebellum reference tissue as per the Centiloid Project methodology.[49] A negative amyloid status was characterized by a cortical ^{11}C-PiB SUVR < 1.21 obtained by converting the Centiloid cut-off of 19 to SUVR using the Centiloid-to-SUVR transformation in Jack *et al.*[50]

Statistical analyses

We compared demographic and clinical variables between the diagnostic groups using analysis of covariance (ANCOVA), and chi-square tests where appropriate. We used a linear mixed effects model to assess the overall relationship between ^{18}F-AV-1451 and ^{11}C-UCB-J BP_{ND}, with age and scan interval as covariates. To adjust for normal levels of tracer uptake from off-target binding not present in the reference region (over and above the correction for non-specific binding in the reference region), we normalized the patient BP_{ND} data against controls by subtracting the regional mean BP_{ND} values in controls from the data of each patient, for each region, for each tracer. Furthermore, we removed regions with previously reported off-target binding of ^{18}F-AV-1451 (basal ganglia and substantia nigra[51]) The linear mixed effect model therefore included normalized ^{11}C-UCB-J as the dependent variable, normalized ^{18}F-AV-1451 as the independent variable, and age and scan interval as covariates of no interest. To investigate the effect of individual variability on the relationship between ^{11}C-UCB-J and ^{18}F-AV-1451 BP_{ND}, we used a linear model with the slope of ^{11}C-UCB-J BP_{ND} as a function of ^{18}F-AV-1451 BP_{ND} for each individual (extracted from the previous linear mixed effect model) as the dependent variable, the PSP rating scale (a measure of disease severity) as the independent variable and age as a covariate of no interest. To explore the correlation between ^{11}C-UCB-J and ^{18}F-AV-1451 BP_{ND} between regions, we calculated a correlation matrix between cortical ^{18}F-AV-1451 binding and synaptic density in cortical and subcortical regions.

Analyses were performed with and without GTM partial volume correction, yielding similar results; we focus on partial volume-corrected BP_{ND} to limit the potential effect of atrophy on our ligand cross-correlation, but present data without PVC in the Supplementary material. Statistical analyses were implemented in R (version 3.6.2).

Data availability

The data that support the findings of this study are available from the corresponding author, upon reasonable request for academic (non-commercial) purposes, subject to restrictions required to preserve participant confidentiality.

Results

Demographics

The patients (PSP and CBD) and control groups were similar in age, sex, education and injected activity of ^{11}C-UCB-J and ^{18}F-AV-1451 (Table 1). We observed typical cognitive profiles for people with PSP and CBD: impaired on verbal fluency, memory and visuospatial domains of the ACE-R, MMSE and INECO frontal screening tool.

Relationship between ^{11}C-UCB-J BP_{ND} and ^{18}F-AV-1451 BP_{ND}

Compared to controls, patients had significantly higher ^{18}F-AV1451 binding in the caudate nucleus, pallidum, putamen and substantia surviving correction for multiple comparison [$P < 0.05$, false discovery rate (FDR) corrected; Supplementary Fig. 1A and Supplementary Table 2]. As previously reported in a smaller cohort,[7,8] patients had significantly lower ^{11}C-UCB-J binding across all cortical and subcortical areas compared to controls, which survived FDR correction (Supplementary Fig. 1B and Supplementary Table 4). Summary statistics for regional ^{18}F-AV1451 and ^{11}C-UCB-J binding potentials in patients and controls are shown in Supplementary Tables 1 and 3, respectively.

There was an overall positive relationship between normalized ^{18}F-AV-1451 BP_{ND} and ^{11}C-UCB-J BP_{ND} across the patient cohort ($\beta = 0.4$, $t = 3.6$, $P = 0.001$; Fig. 2A). There was a significant region × ^{18}F-AV-1451 interaction ($P < 0.001$) driven by subregions of the frontal, parietal and temporal cortices, as well as the hippocampus, subcallosal area and the thalamus, with all but the

hippocampus surviving correction for multiple comparison. Age ($P = 0.9$) and scan interval ($P = 0.5$) did not have a significant effect on the overall model (note that brain regions with known off-target binding of ^{18}F-AV-1451 were removed before running this linear mixed model). The direction of the relationship between ^{18}F-AV-1451 BP_{ND} and ^{11}C-UCB-J BP_{ND} within each individual (i.e. the slope of each grey line in Fig. 2A) negatively correlated with disease severity ($\beta = -0.02$, $t = -2.9$, $P = 0.007$, $R = -0.41$), independent of age (effect of age: $\beta = 0.02$, $t = 2.6$, $P = 0.01$; Fig. 2B). In other words, those patients with more severe disease displayed a less-positive relationship between ^{18}F-AV-1451 BP_{ND} and ^{11}C-UCB-J BP_{ND}.

Of note, the positive correlation between ^{18}F-AV-1451 BP_{ND} and ^{11}C-UCB-J BP_{ND} across the patient cohort remains even if BP_{ND} values are not normalized against the control data ($\beta = 0.4$, $t = 4.0$, $P = 0.0001$), as well as the negative relationship between disease severity and the slope of each individual in Fig. 2A. Also note that similar findings were observed using BP_{ND} derived from data without partial volume correction (Supplementary Fig. 2).

The relationship between ^{18}F-AV-1451 and ^{11}C-UCB-J binding was also positive in an analogous linear mixed effect model in controls alone ($\beta = 0.6$, $t = 4$, $P < 0.0001$), with no main effect of age or scan interval, or ^{18}F-AV-1451 × Region interaction. The relationship between unadjusted ^{18}F-AV-1451 and ^{11}C-UCB-J binding in all three groups (controls, amyloid-negative CBS and PSP) is shown in Supplementary Fig. 3.

Cross-regional correlation between ^{18}F-AV-1451 BP_{ND} and ^{11}C-UCB-J BP_{ND}

Synaptic density in a region is proposed to be affected by both local tau pathology and tau burden in connected regions from which it receives afferent projections. As a result, despite a positive correlation at a regional level, the synaptic density in any given region may be negatively affected by remote insult, with diaschisis between anatomically connected regions (illustrated schematically in Fig. 1A). As an exploratory analysis, we computed the asymmetric Pearson's correlation matrix shown in Fig. 3, between normalized cortical ^{18}F-AV-1451 BP_{ND} (horizontal axis of matrix) and normalized cortical and subcortical ^{11}C-UCB-J BP_{ND} (vertical axis of matrix) in patients. We show that, overall, there are significant negative correlations between cortical (frontal, temporal, parietal, occipital) ^{18}F-AV-1451 BP_{ND} and subcortical ^{11}C-UCB-J BP_{ND} within the caudate nucleus and putamen ($-0.52 < R < -0.37$; $P < 0.05$; uncorrected for multiple comparisons). We observed a positive correlation between ^{18}F-AV-1451 BP_{ND} and ^{11}C-UCB-J BP_{ND} within the thalamus where strong local connections exist (Fig. 3). We did not include subcortical ^{18}F-AV-1451 BP_{ND} in the matrix in Fig. 3 given the off-target binding in these regions, which undermines the interpretability of the signal. However, we include these regions as well as other subregions in the larger correlation matrix in Supplementary Fig. 4 for completeness. Similar findings are seen using BP_{ND} from data without partial volume correction (Supplementary Fig. 5).

Discussion

We have identified an *in vivo* relationship between molecular pathology (estimated with ^{18}F-AV-1451 PET) and synaptic density (estimated with ^{11}C-UCB-J PET) in patients with the primary tauopathies of PSP and CBD (inferred *in vivo* from amyloid-negative CBS). There are three principal results: (i) regions with higher synaptic density have higher molecular pathology; (ii) within regions, synaptic density becomes less dependent on ^{18}F-AV-1451 binding as disease severity increases; and (iii) between regions, increased cortical ^{18}F-AV-1451 binding is associated with reduced subcortical synaptic density. We interpret these three findings in the context of synaptic connectivity-based susceptibility to tauopathy, the synaptotoxic effects of tauopathy and cortico-subcortical diaschisis, respectively. The above results are congruent with the model of tau-induced synaptic toxicity, acknowledging the caveat of off-target binding of ^{18}F-AV-1451. Our primary pathology of interest in the context of PSP and CBD is 4R-tau, but other tauopathies such as latent Alzheimer pathology in older adults and non-tau molecular pathologies may also contribute to ^{18}F-AV-1451 binding.

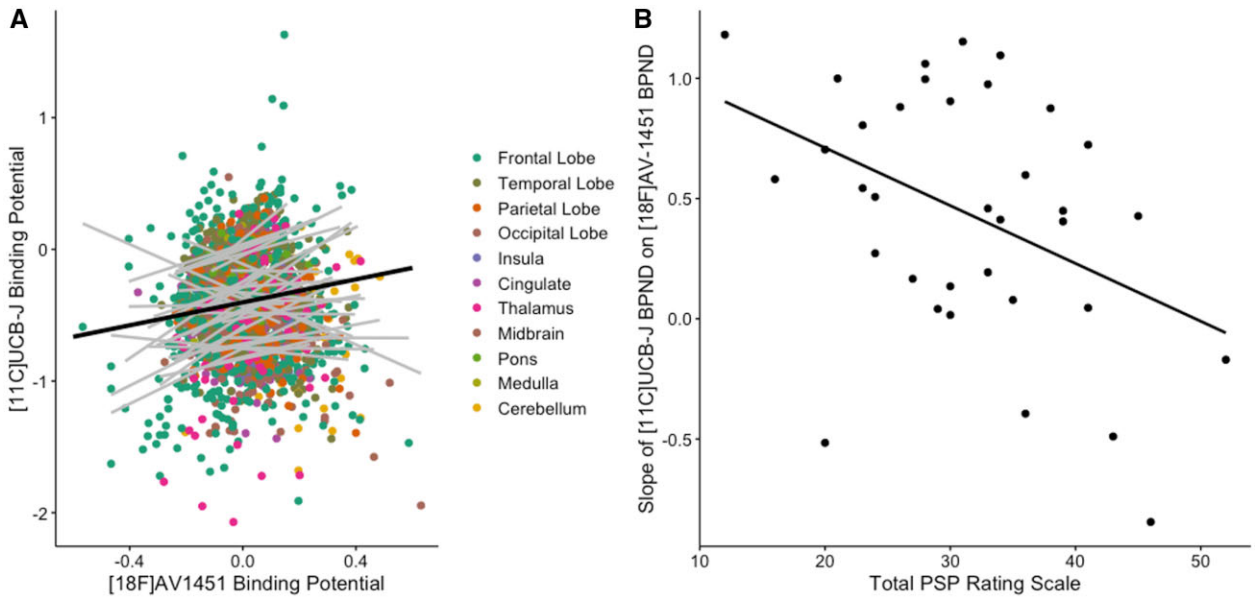

Figure 2 The association between normalized synaptic density (^{11}C-UCB-J) and molecular pathology (^{18}F-AV-1451) is a function of disease severity. (**A**) Scatter plot of ^{11}C-UCB-J BP_{ND} and ^{18}F-AV-1451 BP_{ND} from 35 patients with PSP–Richardson's syndrome and amyloid-negative CBS (each grey line represents a patient), across 73 regions of interest (excluding those with previously reported off-target binding, i.e. basal ganglia and substantia nigra) normalized against controls; the dark black line in **A** depicts the overall fit of the linear mixed model, while grey lines represent individual patient data. (**B**) The slope for each individual (i.e. each grey line in **A**) is negatively correlated with disease severity (as measured with the PSP rating scale); $R = -0.41$, $P < 0.007$.

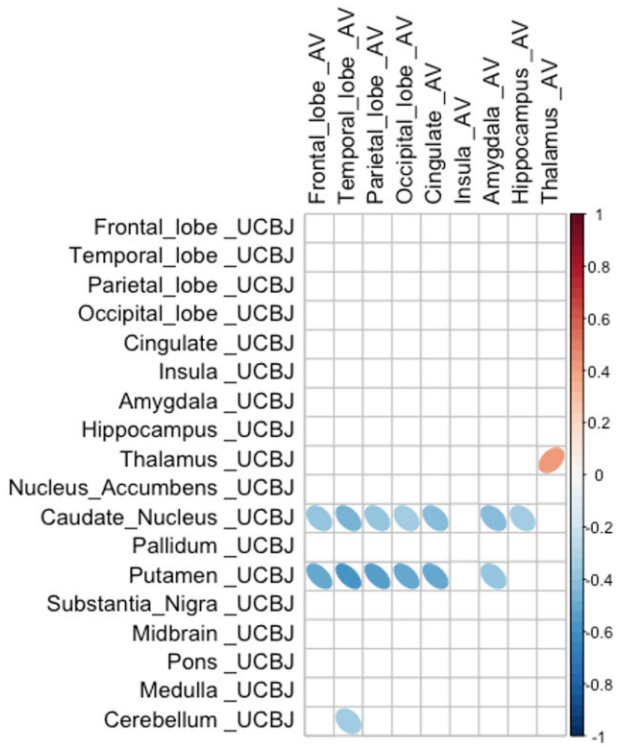

Figure 3 Cortical pathology is negatively correlated with subcortical synaptic density. Correlation, in patients, between normalized ^{18}F-AV-1451 BP_{ND} in cortical regions (horizontal axis) and normalized ^{11}C-UCB-J BP_{ND} in cortical and subcortical target regions (vertical axis). Negative correlations are observed between cortical ^{18}F-AV-1451 BP_{ND} (in frontal, temporal, parietal and occipital cortices), and ^{11}C-UCB-J BP_{ND} in the caudate nucleus, putamen and cerebellum. Only significant correlations (at $P < 0.05$ uncorrected for multiple comparisons) are shown.

The effect of hyperphosphorylated tau on synaptic function and density is complex. It involves both direct and indirect pathways of injury with changes in cellular physiology preceding the loss of neurons. Through direct pathways, pathological tau interferes with dendritic morphology, synaptic protein expression, the number of NMDA (*N*-methyl-D-aspartate) and AMPA (α-amino-3-hydroxy-5-methyl-4-isoxazolepropionic acid) receptors on the presynaptic membrane, mitochondrial function, synaptic vesicle numbers and ultimately synaptic loss (for a review of animal studies illustrating various direct tau-induced synaptic abnormalities, see Jadhav *et al.*[52]). Tau also directly affects the axon cytoskeleton and trafficking, as well as the normal functioning of the soma.[53] Indirectly, hyperphosphorylated tau adversely affects the functioning of the neuronal support network, including glia cells and astrocytes.[54–56] These events are affected by the stage and severity of the disease process, and in relation to regional differences in connectivity which we discuss next (concepts schematically illustrated in Fig. 1).

We identified a positive relationship between the binding of ^{11}C-UCB-J and ^{18}F-AV-1451 such that areas of the brain with higher synaptic density had higher molecular pathology. This accords with preclinical and clinical models of tauopathy in which the strength of local network connectivity facilitates the transneuronal spread of tau pathology.[9,12,57–59]

However, the relationship between tau accumulation and synaptic density changes with disease progression, at least as inferred from the cross-sectional moderation by disease severity (Fig. 2B). With increasing scores on the PSP rating scale, synaptic density becomes less dependent on local accumulation of pathology. In other words, according to the model (Fig. 1) in areas with relatively low tau accumulation synaptic density is minimally affected, whereas in areas with higher tau accumulation there is reduction of synaptic density as the disease progresses, and this preferentially occurs in synapse-rich areas. As the disease progresses, other pathological processes may contribute to synaptic loss, such as inflammation, another predictor of prognosis and mediator of synaptic loss.[60] Therefore, there is not a simple linear relationship between tau accumulation and synaptic density in moderate and advanced disease. This observation accords with human post-mortem and animal studies. In post-mortem studies of the tauopathy Alzheimer's disease, there is a biphasic synaptic protein response during disease progression, with increases in synaptophysin/syntaxin/SNAP-25 in early Braak stages and synaptic loss observed only when the disease has progressed to the neocortex.[19] In the P301L transgenic mouse model of PSP-like tauopathy, there is a differential loss of synapses, as well as synaptic proteins, depending on disease stage.[20] These results have recently been replicated *in vivo*, where the relationship between synaptic density and tau burden in patients with Alzheimer's disease is reported to be modulated by cortical tau load. Coomans *et al.*[22] show that in patients with mild disease and low cortical tau burden, the relationship between tau and synaptic density is positive, whereas in those with increasing cortical tau load, this relationship changes direction; the relationship between the two tracers in controls is not reported.

In our study, we also observe a positive relationship between ^{18}F-AV-1451 and ^{11}C-UCB-J binding potentials in controls (Supplementary Fig. 3), even though ^{18}F-AV-1451 binding is lower in controls. Disease-related ^{18}F-AV-1451 binding attributable to presence of PSP/CBD pathology is unlikely in the controls, as the prevalence of these conditions in the normal population is only 1/10 000.[61] However, the presence of asymptomatic Alzheimer's disease pathology in the normal older population is more likely. Rising from the age of 40, by the age of 85 two-thirds of cognitively normal individuals will show positive changes in the A/T/N classification for Alzheimer's disease, whether by CSF, plasma or amyloid PET.[62,63] Some of the non-specific ^{18}F-AV-1451 signal, even in healthy controls, may therefore be attributable to latent/preclinical Alzheimer's disease pathology. We control for this component of the signal by subtracting the mean regional control values from those of the patients.

The positive correlation between ^{18}F-AV-1451 and ^{11}C-UCB-J binding potential in controls appears stronger compared to that seen in patients, as a group (Supplementary Fig. 3). One explanation for this observation is the heterogeneity in disease severity in PSP/CBD, given the interaction between ^{11}C-UCB-J, ^{18}F-AV-1451 and disease severity. This can be understood in terms of the model set out in Fig. 1. The patient group includes those with a strong positive correlation (at early stages of disease) and those with negligible correlation (as a consequence of more advanced disease). The net result for a group-wise test will be a reduction of the group correlation. This is not present in the control group, in whom the level of tau pathology is expected to be very much lower (even if present from Alzheimer type tau with high ^{18}F-AV-1451 affinity).

To understand the biphasic relationship between molecular pathology and synaptic density, one must consider other key players in synaptotoxicity in tauopathies, such as neuroinflammation.[64] Recent *in vivo* studies have confirmed the regional co-localization of inflammation and ^{18}F-AV-1451 binding in PSP, including in many cortical areas,[65] in line with previous *in vivo*[66,67] and post-mortem[68] reports of the tight interplay between neuroinflammation and tau accumulation in tauopathies. There is growing evidence that these two pathological processes affect synaptic function both independently and synergistically.

The relationship between tauopathy and synaptic density is even more intriguing when considering the change in synaptic density in one region as a function of pathology in another. There are strong correlations between ^{11}C-UCB-J binding within the basal ganglia (in particular the caudate nucleus and putamen) and ^{18}F-AV-1451 binding in all major cortical areas. The reverse association, between subcortical ^{18}F-AV-1451 and cortical ^{11}C-UCB-J binding is also observed (Supplementary Figs 4 and 5) but is dismissed here as uninterpretable in view of subcortical off-target binding of ^{18}F-AV-1451. The significant negative correlation between cortical ^{18}F-AV-1451 binding and synaptic density in the basal ganglia could be a reflection of severe disease in the basal ganglia and accumulating pathology in the neocortex. In other words, synapses are severely affected in the basal ganglia as one of the earliest sites of pathology, with pathology spreading and accumulating in synapse-rich areas of the brain, for example the neocortex. A second possible explanation is that loss of descending cortico-striatal axons due to cortical pathology may cause diaschisis, affecting subcortical synaptic density even further. Previous analysis of diffusion tensor imaging in patients with PSP/CBD have revealed extensive white matter abnormalities (within the main association fibres) beyond the degree of cortical atrophy,[69,70] resulting in loss of cortical afferents onto subcortical structures. A third, although not mutually exclusive, potential explanation is the weakening of cortical–subcortical functional connectivity resulting from dysfunctional synapses rather than synaptic loss, although cortico-subcortical connectivity is inferred and was not directly measured in our study.

Although at a regional level there is a positive correlation between ^{11}C-UCB-J and ^{18}F-AV-1451 BP_{ND}, we are not directly measuring either synaptic function or the synaptotoxic tau oligomers. This caveat must be borne in mind when interpreting PET data. It is the preclinical models that have shown that oligomers of tau are toxic to synaptic function, even in the absence of tau polymers/fibrils.[15,16] By the time tau aggregates are established, oligomers of tau are expected cortically, and perhaps interfere with cortical function and the integrity of descending axons.

There are other limitations to our study. First, the low affinity of ^{18}F-AV-1451 for PSP and CBD 4R tau. Even though the radioligand recapitulates the distribution of post-mortem neuropathology in PSP and CBD and binds PSP 4R tau, the affinity is very much lower than for 3R tau in Alzheimer's disease. Second, there is well-established off-target binding of ^{18}F-AV-1451, particularly within subcortical structures where monoamine oxidase and neuromelanin are present. Off-target binding is most prominent in the basal ganglia and substantia nigra, which we excluded before running the linear mixed model and correlation matrix. We included these regions in the detailed descriptive correlation matrices in Supplementary Figs 4 and 5 for completeness sake, noting the strong negative correlations between cortical ^{18}F-AV-1451 BP_{ND} and subcortical ^{11}C-UCB-J BP_{ND}. Furthermore, we normalized our patient data against those of controls to remove any additional normal levels of off-target binding, noting the caveat that the remaining signal in patients may still arise from tau and non-tau pathology; there is no evidence to suggest that ^{18}F-AV-1451 shares a common binding target with ^{11}C-UCB-J, which has a high specificity for SV2A in previous *in vivo* and *in vitro* validation studies.[38,71] Third, we note that in PET studies of neurodegeneration with atrophy, grey matter volume loss can affect the interpretation of PET signals. However, synaptic loss in PSP and CBD occurs even in areas of the brain without discernible atrophy on MRI.[7,8] Nonetheless, we used a stringent partial volume correction method (GTM) to minimize the effect of atrophy on our ligand cross-correlations. Of note, our data without partial volume correction yield similar results in all the main analyses (Supplementary Figs 2 and 5). Fourth, although the sample size is small, it is adequately powered in view of the large effect sizes seen. However, more subtle relationships with phenotypic variants of PSP and CBS would require larger studies. Additionally, clinical diagnostic criteria for PSP–Richardson's syndrome and amyloid-negative CBS (here called CBD) were used to select a clinical cohort with likely a 4R-tauopathy as the underlying pathological diagnosis. While both PSP–Richardson's syndrome and amyloid-negative CBS are highly correlated with a 4R-tauopathy at post-mortem, both from our local brain bank and internationally,[26,27,72] other pathologies are possible, and so are coexistent pathologies that may synergistically contribute to neurodegeneration.[73] Neuropathological correlates, to test the correlations between phenotype and pathology, and between *in vivo* to post-mortem measures of synaptic density, as well as tau to synapse correlations would be useful but are not yet available for our cohort. Lastly, the cross-sectional design of this study limits the interpretation of the dynamic relationship between pathology and synaptic loss. Although we include patients at various stages of their illness, a longitudinal design is necessary to test the dynamic relationship we propose and the mediation of synaptic loss by progressive tauopathy.

In conclusion, we demonstrate a widespread positive association between ^{18}F-AV-1451 and ^{11}C-UCB-J binding in patients with symptomatic PSP and amyloid-negative CBS. Individual variability in this association correlates with disease severity. The complex relationship between molecular pathology, including but not exclusive to tau, and synaptic density may explain changes in cognitive and motor physiology. We hope that these insights will inform the design of new clinical trials to arrest PSP and CBD.

Acknowledgements

The authors thank the research participants and caregivers, the staff at the Wolfson Brain Imaging Centre, and at the Cambridge Centre for Parkinson-Plus. We thank the NIHR Cambridge Biomedical Research Centre for support. We thank UCB Pharma, and Avid (Lilly) for providing the precursor for ^{11}C-UCB-J and ^{18}F-AV-1451 synthesis, respectively. N.H. and J.B.R. had full access to all the data in the study and take responsibility for the integrity of the data and the accuracy of the data analysis. The view expressed are those of the authors and not necessarily those of the NIHR or the Department of Health and Social Care. For the purpose of open access, the author has applied a CC BY public copyright licence to any Author Accepted Manuscript version arising from this submission.

Funding

The study was funded by the Wellcome Trust (220258), Cambridge Centre for Parkinson-Plus (RG95450); the National Institute for Health Research Cambridge Biomedical Research Centre (BRC-1215–20014); the PSP Association ('MAPT-PSP' study), Medical Research Council (SUAG/051 G101400), and the Association of British Neurologists, Patrick Berthoud Charitable Trust (RG99368).

Competing interests

J.B.R. serves as an associate editor to *Brain* and is a non-remunerated trustee of the Guarantors of Brain, Darwin College and the PSP Association (UK). He provides consultancy to Asceneuron, Biogen, UCB, Astex, WAVE, Curasen, SV Health and has research grants from AZ-Medimmune, Janssen, Lilly as industry partners in the Dementias Platform UK. J.T.O. has no conflicts related to this study. Unrelated to this work he has received honoraria for work

as DSMB chair or member for TauRx, Axon, Eisai, has acted as a consultant for Roche, has received research support from Alliance Medical and Merck. T.R. has received honoraria from Biogen and the National Institute for Health and Clinical Excellence (NICE). No other conflict of interest is reported by other authors.

References

1. Bigio EH, Vono MB, Satumtira S, et al. Cortical synapse loss in progressive supranuclear palsy. *J Neuropathol Exp Neurol*. 2001; 60(5):403–410.
2. Lipton AM, Cullum CM, Satumtira S, et al. Contribution of asymmetric synapse loss to lateralizing clinical deficits in frontotemporal dementias. *Arch Neurol*. 2001;58(8):1233–1239.
3. Clare R, King VG, Wirenfeldt M, Vinters HV. Synapse loss in dementias. *J Neurosci Res*. 2010;88(10):2083–2090.
4. DeKosky ST, Scheff SW. Synapse loss in frontal cortex biopsies in Alzheimer's disease: Correlation with cognitive severity. *Ann Neurol*. 1990;27(5):457–464.
5. Terry RD, Masliah E, Salmon DP, et al. Physical basis of cognitive alterations in Alzheimer's disease: Synapse loss is the major correlate of cognitive impairment. *Ann Neurol*. 1991;30(4): 572–580.
6. Jacobsen JS, Wu C-C, Redwine JM, et al. Early-onset behavioral and synaptic deficits in a mouse model of Alzheimer's disease. *Proc Natl Acad Sci U S A*. 2006;103:5161–5166.
7. Mak E, Holland N, Jones PS, et al. *In vivo* coupling of dendritic complexity with presynaptic density in primary tauopathies. *Neurobiol Aging*. 2021;101:187–198.
8. Holland N, Jones PS, Savulich G, et al. Synaptic loss in primary tauopathies revealed by [^{11}C]UCB-J positron emission tomography. *Mov Disord*. 2020;35(10):1834–1842.
9. Ahmed Z, Cooper J, Murray TK, et al. A novel *in vivo* model of tau propagation with rapid and progressive neurofibrillary tangle pathology: The pattern of spread is determined by connectivity, not proximity. *Acta Neuropathol*. 2014;127(5):667–683.
10. Liu L, Drouet V, Wu JW, et al. Trans-synaptic spread of tau pathology *in vivo*. *PLoS One*. 2012;7(2):e31302.
11. DeVos SL, Corjuc BT, Oakley DH, et al. Synaptic tau seeding precedes tau pathology in human Alzheimer's Disease brain. *Front Neurosci* 2018;12:267.
12. Polanco JC, Li C, Durisic N, Sullivan R, Götz J. Exosomes taken up by neurons hijack the endosomal pathway to spread to interconnected neurons. *Acta Neuropathol Commun* 2018;6(1):10.
13. Gibbons GS, Lee VMY, Trojanowski JQ. Mechanisms of cell-to-cell transmission of pathological tau: A review. *JAMA Neurol*. 2019;76(1):101–108.
14. Seemiller J, Bischof GN, Hoenig MC, Tahmasian M, van Eimeren T, Drzezga A.; Alzheimer's Disease Neuroimaging Initiative. Indication of retrograde tau spreading along Braak stages and functional connectivity pathways. *Eur J Nucl Med Mol Imaging*. 2021;48(7):2272–2282.
15. Menkes-Caspi N, Yamin HG, Kellner V, Spires-Jones TL, Cohen D, Stern EA. Pathological tau disrupts ongoing network activity. *Neuron*. 2015;85(5):959–966.
16. Kaniyappan S, Chandupatla RR, Mandelkow EM, Mandelkow E. Extracellular low-n oligomers of tau cause selective synaptotoxicity without affecting cell viability. *Alzheimer's Dement*. 2017; 13(11):1270–1291.
17. Jiang S, Wen N, Li Z, et al.; International FTD-Genomics Consortium (IFGC). Integrative system biology analyses of CRISPR-edited iPSC-derived neurons and human brains reveal deficiencies of presynaptic signaling in FTLD and PSP. *Transl Psychiatry*. 2018;8(1):265.
18. Spires-Jones, TL, Hyman, BT. The intersection of amyloid beta and tau at synapses in Alzheimer's disease. *Neuron*. 2014;82:756–771.
19. Mukaetova-Ladinska EB, Garcia-Siera F, Hurt J, et al. Staging of cytoskeletal and β-amyloid changes in human isocortex reveals biphasic synaptic protein response during progression of Alzheimer's disease. *Am J Pathol*. 2000;157(2):623–636.
20. Kopeikina KJ, Polydoro M, Tai HC, et al. Synaptic alterations in the rTg4510 mouse model of tauopathy. *J Comp Neurol*. 2013; 521(6):1334–1353.
21. Vanhaute H, Ceccarini J, Michiels L, et al. *In vivo* synaptic density loss is related to tau deposition in amnestic mild cognitive impairment. *Neurology*. 2020;95(5):e545–e553.
22. Coomans EM, Schoonhoven DN, Tuncel H, et al. *In vivo* tau pathology is associated with synaptic loss and altered synaptic function. *Alzheimer's Res Ther*. 2021;13:35.
23. Malpetti M, Kievit RA, Passamonti L, et al. Microglial activation and tau burden predict cognitive decline in Alzheimer's disease. *Brain*. 2020;143(5):1588–1602.
24. Höglinger GU, Respondek G, Stamelou M, et al.; for the Movement Disorder Society-endorsed PSP Study Group. Clinical diagnosis of progressive supranuclear palsy: The movement disorder society criteria. *Mov Disord*. 2017;32(6):853–864.
25. Armstrong MJ, Litvan I, Lang AE, et al. Criteria for the diagnosis of corticobasal degeneration. *Neurology*. 2013;80(5):496–503.
26. Alexander SK, Rittman T, Xuereb JH, Bak TH, Hodges JR, Rowe JB. Validation of the new consensus criteria for the diagnosis of corticobasal degeneration. *J Neurol Neurosurg Psychiatry*. 2014;923–927.
27. Gazzina S, Respondek G, Compta Y, et al. Neuropathological validation of the MDS-PSP criteria with PSP and other frontotemporal lobar degeneration. *bioRxiv: Cold Spring Harbor Laboratory*. 2019; 520510.
28. Dickson DW, Kouri N, Murray ME, Josephs KA. Neuropathology of frontotemporal lobar degeneration-tau (FTLD-tau). *J Mol Neurosci*. 2011;45(3):384–389.
29. Kovacs GG, Lukic MJ, Irwin DJ, et al. Distribution patterns of tau pathology in progressive supranuclear palsy. *Acta Neuropathol*. Aug 2020;140(2):99–119.
30. Zhou L, McInnes J, Wierda K, et al. Tau association with synaptic vesicles causes presynaptic dysfunction. *Nat Commun*. 2017; 8(1):15295.
31. Josephs KA, Whitwell JL, Tacik P, et al. [^{18}F]AV-1451 tau-PET uptake does correlate with quantitatively measured 4R-tau burden in autopsy-confirmed corticobasal degeneration. *Acta Neuropathologica*. 2016;132(6):931–933.
32. Smith R, Puschmann A, Schöll M, et al. ^{18}F-AV-1451 tau PET imaging correlates strongly with tau neuropathology in MAPT mutation carriers. *Brain*. 2016;139(Pt 9):2372–2379.
33. Whitwell JL, Lowe VJ, Tosakulwong N, et al. [^{18}F]AV-1451 tau positron emission tomography in progressive supranuclear palsy. *Mov Disord*. 2017;32(1):124–133.
34. Ono M, Sahara N, Kumata K, et al. Distinct binding of PET ligands PBB3 and AV-1451 to tau fibril strains in neurodegenerative tauopathies. *Brain*. 2017;140(3):764–780.
35. Ali F, Whitwell JL, Martin PR, et al. [^{18}F] AV-1451 uptake in corticobasal syndrome: The influence of beta-amyloid and clinical presentation. *J Neurol*. 2018;265(5):1079–1088.
36. Soleimani-Meigooni DN, Iaccarino L, La Joie R, et al. ^{18}F-flortaucipir PET to autopsy comparisons in Alzheimer's disease and other neurodegenerative diseases. *Brain*. 2020;143(11): 3477–3494.
37. Goodheart AE, Locascio JJ, Samore WR, et al. ^{18}F-AV-1451 positron emission tomography in neuropathological substrates of corticobasal syndrome. *Brain*. 2021;144(1):266–277.

38. Finnema SJ, Nabulsi NB, Eid T, et al. Imaging synaptic density in the living human brain. *Sci Transl Med*. 2016;8(348):348ra96.
39. Bajjalieh SM, Peterson K, Linial M, Scheller RH. Brain contains two forms of synaptic vesicle protein 2. *Proc Natl Acad Sci U S A*. 1993;90(6):2150–2154.
40. Lang AE, Stebbins GT, Wang P, et al.; PROSPECT-M-UK investigators. The Cortical Basal ganglia Functional Scale (CBFS): Development and preliminary validation. *Parkinson Related Disord*. 2020;79:121–126.
41. Burgos N, Cardoso MJ, Thielemans K, et al. Attenuation correction synthesis for hybrid PET-MR scanners: Application to brain studies. *IEEE Trans Med Imaging*. 2014;33(12):2332–2341.
42. Manavaki R, Hong Y, Fryer TD. Brain MRI coil attenuation map processing for the GE SIGNA PET/MR: Impact on PET image quantification and uniformity. In: *IEEE Nuclear Science Symposium and Medical Imaging Conference Proceedings*; 2019.
43. Avants BB, Epstein CL, Grossman M, Gee JC. Symmetric diffeomorphic image registration with cross-correlation: Evaluating automated labeling of elderly and neurodegenerative brain. *Med Image Anal*. 2008;12(1):26–41.
44. Rousset OG, Ma Y, Evans AC. Correction for partial volume effects in PET: Principle and validation. *J Nucl Med*. 1998;39(5): 904–911.
45. Wu Y, Carson RE. Noise reduction in the simplified reference tissue model for neuroreceptor functional imaging. *J Cereb Blood Flow Metab*. 2002;22(12):1440–1452.
46. Koole M, van Aalst J, Devrome M, et al. Quantifying SV2A density and drug occupancy in the human brain using [^{11}C]UCB-J PET imaging and subcortical white matter as reference tissue. *Eur J Nucl Med Mol Imaging*. 2019;46(2):396–406.
47. Rossano S, Toyonaga T, Finnema SJ, et al. Assessment of a white matter reference region for 11C-UCB-J PET quantification. *J Cerebral Blood Flow Metabol*. 2020;40(9):1890–1901.
48. Gunn RN, Lammertsma AA, Hume SP, Cunningham VJ. Parametric imaging of ligand–receptor binding in PET using a simplified reference region model. *NeuroImage*. 1997;6(4):279–287.
49. Klunk WE, Koeppe RA, Price JC, et al. The Centiloid project: Standardizing quantitative amyloid plaque estimation by PET. *Alzheimer's Dement*. 2015;11(1):1–15.e154.
50. Jack CR, Wiste HJ, Weigand SD, et al. Defining imaging biomarker cut points for brain aging and Alzheimer's disease. *Alzheimer's Dement*. 2017;13(3):205–216.
51. Leuzy, A, Chiotis, K, Lemoine, L, et al. Tau PET imaging in neurodegenerative tauopathies—Still a challenge. *Mol Psychiatry*. 2019:1112–1134.
52. Jadhav S, Cubinkova V, Zimova I, et al. Tau-mediated synaptic damage in Alzheimer's disease. *Transl Neurosci*. 2015;6(1):214–226.
53. Kneynsberg, A, Combs, B, Christensen, K, Morfini, G, Kanaan, NM. Axonal degeneration in tauopathies: Disease relevance and underlying mechanisms. *Front Neurosci*. 2017;11:572.
54. Vogels T, Murgoci AN, Hromádka T. Intersection of pathological tau and microglia at the synapse. *Acta Neuropathol Commun*. 2019;7(1):109.
55. Kovacs GG. Astroglia and tau: New perspectives. *Front Aging Neurosci*. 2020;12:96.
56. Casaletto KB, Zetterberg H, Blennow K, et al. Tripartite relationship among synaptic, amyloid, and tau proteins: An *in vivo* and postmortem study. *Neurology*. 2021;97(3):e284.
57. Clavaguera F, Bolmont T, Crowther RA, et al. Transmission and spreading of tauopathy in transgenic mouse brain. *Nat Cell Biol*. 2009;11(7):909–913.
58. Clavaguera F, Akatsu H, Fraser G, et al. Brain homogenates from human tauopathies induce tau inclusions in mouse brain. *Proc Natl Acad Sci U S A* 2013;110(23):9535–9540.
59. Cope TE, Rittman T, Borchert RJ, et al. Tau burden and the functional connectome in Alzheimer's disease and progressive supranuclear palsy. *Brain*. 2018;141(2):550–567.
60. Malpetti M, Passamonti L, Jones PS, et al. Neuroinflammation predicts disease progression in progressive supranuclear palsy. *J Neurol Neurosurg Psychiatry*. 2021;92(7):769–325549.
61. Coyle-Gilchrist ITS, Dick KM, Patterson K, et al. Prevalence, characteristics, and survival of frontotemporal lobar degeneration syndromes. *Neurology*. 2016;86(18):1736–1743.
62. Toledo JB, Zetterberg H, van Harten AC, et al.; Alzheimer's Disease Neuroimaging Initiative. Alzheimer's disease cerebrospinal fluid biomarker in cognitively normal subjects. *Brain*. 2015;138(Pt 9):2701–2715.
63. Tissot C. L., Benedet, A, Therriault, J, et al.; Alzheimer's Disease Neuroimaging Initiative. Plasma pTau181 predicts cortical brain atrophy in aging and Alzheimer's disease. *Alzheimer's Res Ther*. 2021;13(1):69.
64. Palleis C, Sauerbeck J, Beyer L, et al. *In vivo* assessment of neuroinflammation in 4-repeat tauopathies. *Mov Disord*. 2021;36(4): 883–894.
65. Malpetti M, Passamonti L, Rittman T, et al. Neuroinflammation and tau colocalize *in vivo* in progressive supranuclear palsy. *Ann Neurol*. 2020;88(6):1194–1204.
66. Gerhard A, Trender-Gerhard I, Turkheimer F, Quinn NP, Bhatia KP, Brooks DJ. *In vivo* imaging of microglial activation with [^{11}C]-PK11195 PET progresive supranuclear palsy. *Mov Disord*. 2006; 21(1):89–93.
67. Gerhard A, Watts J, Trender-Gerhard I, et al. *In vivo* imaging of microglial activation with [^{11}C] (R)–PK11195 PET in corticobasal degeneration. *Mov Disord*. 2004;19(10):1221–1226.
68. Metaxas A, Thygesen C, Briting SRR, Landau AM, Darvesh S, Finsen B. Increased inflammation and unchanged density of synaptic vesicle glycoprotein 2A (SV2A) in the postmortem frontal cortex of Alzheimer's disease patients. *Front Cell Neurosci*. 2019;13:538.
69. Borroni B, Garibotto V, Agosti C, et al. White matter changes in corticobasal degeneration syndrome and correlation with limb apraxia. *Arch Neurol*. 2008;65(6):796–801.
70. Padovani A, Borroni B, Brambati SM, et al. Diffusion tensor imaging and voxel based morphometry study in early progressive supranuclear palsy. *J Neurol Neurosurg Psychiatry*. 2006;77(4): 457–463.
71. Nabulsi NB, Mercier J, Holden D, et al. Synthesis and preclinical evaluation of ^{11}C-UCB-J as a PET tracer for imaging the synaptic vesicle glycoprotein 2A in the brain. *J Nucl Med*. 2016;57(5):777–784.
72. Respondek G, Kurz C, Arzberger T, et al.; for the Movement Disorder Society-Endorsed PSP Study Group. Which ante mortem clinical features predict progressive supranuclear palsy pathology? *Mov Disord*. 2017;32(7):995–1005.
73. Robinson JL, Lee EB, Xie SX, et al. Neurodegenerative disease concomitant proteinopathies are prevalent, age-related and APOE4-associated. *Brain*. 2018;141(7):2181–2193.